Journal of Sound and Vibration (2000) **233**(3), 495–514
doi:10.1006/jsvi.1999.2835, available online at http://www.idealibrary.com on IDEAL®

BOUNDARY CONDITION IDENTIFICATION USING CONDENSATION AND INVERSION — APPLICATION TO OPERATING PIPING NETWORK

S. FRIKHA

Laboratoire de Mécanique Physique UPRESA CNRS 7068, *Université Pierre et Marie Curie*, 2 *Pl. de la gare de Ceinture*, 78210 *Saint Cyr l'Ecole*, *France*

G. COFFIGNAL

Laboratoire de Modélisation et de Mécanique des Structures, *UPRESA CNRS* 8007, *Ecole Nationale Supérieure des Arts et Métiers*, 151 *Bd de l'Hôpital* 75013 *Paris*

AND

J. L. TROLLE

Electricité De France, *division R&D*, *département Acoustique et Mécanique Vibratoire*, 1 *Avenue du Général De Gaulle*, 92141 *Clamart*, *France*

(*Received* 18 *June* 1999, *and in final form* 9 *December* 1999)

This paper deals with the experimental analysis of piping systems under operating conditions in the field of vibration and acoustic analysis. A new approach to identify the boundary conditions of a part of a curvilinear structure is presented. The basic concept consists of solving an inverse problem where the measured response of the system tested is combined with an incomplete analytical model in order to identify the boundary dynamical state in the frequency domain. As in finite element methods, the tested network is described using elements and nodes. An original technique using a transfer matrix of continuous elements provides a small-size analytical model. In addition, condensation procedure is used to eliminate all degrees of freedom (d.o.f.) having a modelled boundary condition and to reduce the size of the solved inverse problem. Since identification of boundary conditions is performed, the analysis of dynamic response of the tested network may be performed without further matrix computation. The validity and the feasibility of the approach are shown using actual test results. Examples concerning real applications are also presented.

1. INTRODUCTION

In many cases, the dynamic behaviour of structures and machines is strongly dependent on operating conditions. Besides modifying the excitation forces acting on a system, coupling phenomena inherent to operating conditions may strongly affect the mechanical behaviour of the system. For example, the quality factor and the frequency bandwidth of an acoustic filter may be changed significantly by the effects of a temperature gradient or a turbulent flow. The complexity of such behaviour and the growing need for accuracy makes it necessary to resort to experimental analyses that have to be carried out under operating conditions. This implies that some excitations and some boundary conditions can neither be modelled nor measured.

0022-460X/00/230495 + 20 $35.00/0

On the other hand, inverse methods are specifically used when direct measurements are not possible. The assessment and the reliability of an inverse method generally depend on the size and the complexity of the identified model. For large structure analysis, sub-structur ing allows a significant reduction of the model size and leads to a better conditioned inverse problem. One of the major difficulties encountered in this case is the description of the interface conditions which define part of the boundary conditions for each substructure.

In this context, the present paper is focused on experimental analyses that should be carried out under operating conditions involving unknown boundary conditions. In particu lar, the case of fluid-filled piping networks is investigated [1]. These systems are usually subject to vibro-acoustic and aero-acoustic coupling which are often responsible for poorly understood sources of excitation (as in pumps, valves, internal combustion engines). Moreover, these systems usually constitute large networks which have uncertain behaviour and which may be affected by ageing modifications. An *in situ* diagnostic analysis very often requires experimental analysis only on the part of the piping network where abnormal behaviour is suspected. A typical example is the piping systems of energy production plants which are often several kilometres long and include several singularities.

A brief review of the dominant tendencies of experimental approaches for acoustic and vibration analysis, developed during last decades follows. Three classes of methods may be distinguished. The first class is basically related to the field of the experimental modal analysis. This widely used approach consists of exploiting, in a time or frequency domain, the response of an excited system, in order to extract its modal properties and update its analytical model [2–9]. This requires controlled or modelled boundary conditions. However, recent research is focused on adapting these techniques to operating experimental analyses and thereby overcoming their main limitations. The basic concept consists of using only output data to identify modal properties [10, 11]. Hermans *et al.* [10] show the efficiency of this approach to identify modal parameters (eigenfrequencies, damping ratio, eigenmodes) under working conditions. Nevertheless, it is observed that the assessment of the modal participation factors is conditioned by the whiteness of the unknown excitations acting on the system.

The second class includes methods based on characterization of waves propagating in the tested part of the structure. These approaches are basically developed to perform experimen tal analysis under uncontrolled conditions. They have a local character because wave properties change when they cross any singularity or bifurcation. The wave intensity identification method is the most well known [12–15]. It is based on the use of a sensor array to identify complex wave amplitudes.

The third class includes methods which analyze the measured response as a dynamic signal without associating any mechanical model to the tested system. They are commonly used for dynamic system monitoring and damage detection. These methods provide only global information on the system behaviour (black box) observed from a single or a multiple response.

In this paper, a new hybrid experimental/analytical approach is presented. Similar to methods of the second class, it is basically suitable for uncontrolled conditions such as working system analyses, and like those of the first class, it uses a global analytical model and leads to a detailed analysis. The most significant feature of this study consists of combining a global analytical model and experimental data in order to perform experiment al analysis of dynamic behaviour of a complex structure having unknown boundary conditions. The main purpose is the identification of boundary conditions describing the mechanical links between the part of the system studied and its unknown singularities on the one hand, and the mechanical links between it and the rest of the system on the other.

Classically, a mechanical link is characterized by a generalized displacement or a generalized force. The experimental data consist of the response of a few points of the studied part (displacement, velocity, internal strains, etc.). Curvilinear structures composed of beams, fluid-filled pipes and lumped elements constitute the main application of this study. However, the basic concepts may be applied to other types of structures having linear behaviour. Both the mechanical characteristics of the test part and the location of the unknown boundary conditions are assumed to be well known. The dynamic behaviour of curvilinear elements is expressed using a continuous element formulation which avoids discretization errors, as encountered in finite element models, and allows the use of a minimal number of degrees of freedom. Furthermore, an exact condensation procedure is introduced. It enables the processing of the degrees of freedom having modelled boundary conditions to be separated from the processing of the degrees of freedom having unknown boundary conditions and reduces the size of the inverse problem.

After a detailed presentation of the identification method in the second section, the third section gives some results showing the validity and the feasibility of the applied approach in the field of vibration and acoustic.

2. IDENTIFICATION METHOD

2.1. PRINCIPLE

The case where some of the boundary conditions are unknown is considered. This situation occurs either if only a part of the system is modelled or if the network studied includes singularities having unknown behaviour. Several examples are encountered:

- the vibro-acoustic behaviour of pumps, valves and several regulation systems is often poorly understood under working conditions,
- the supporting structure of pipe networks usually have a complex vibratory behaviour,
- the acoustic behaviour of branch tubes such as pressure pick-ups or side branches provide complex coupling phenomena,
- natural excitations caused by fluid and structure interactions are often difficult to model.

The lack of boundary conditions makes the analysis of the dynamic response of the system an ill-posed problem. The method developed consists of using the measurement of the response at a set of internal points of the system to overcome the lack of data. An inverse problem is then solved where the relationship between measured data and unknown boundary conditions is inverted. This equation is derived from the structure model being tested. The instrumented structure then constitutes a "macro generalized sensor" allowing an experimental assessment of unknown boundary conditions. Figure 1 presents a basic example illustrating the features of the method where the boundary conditions between the tested part and its singularities, those associated with supporting conditions and those corresponding to connections between the studied part and the rest of the network, have to be identified.

Figure 2 summarizes the difference between the direct and inverse problem treated here. A direct problem, classically solved to perform predictive analysis, consists of modelling the boundary conditions of a real system and then computing an estimation of its response using a mathematical model idealizing its behaviour. An inverse problem is generally solved when an identification or a diagnostic analysis are needed. It consists of introducing measured responses to replace the lack of modelling. In the present paper, the known data of the modelled system are a part of the boundary conditions and a part of the system

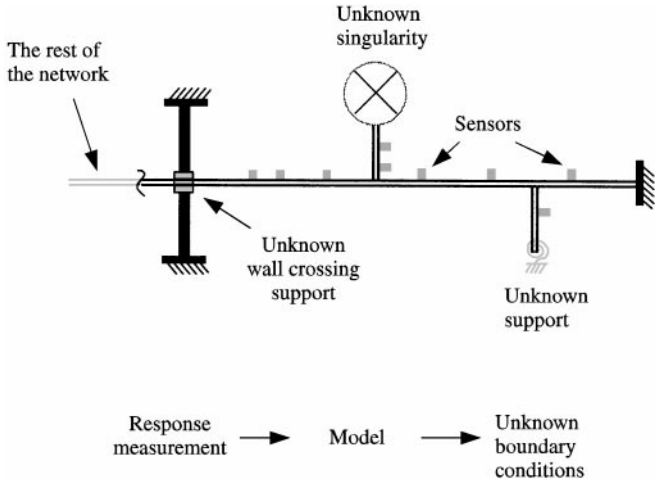

Figure 1. Schematic diagram of the system.

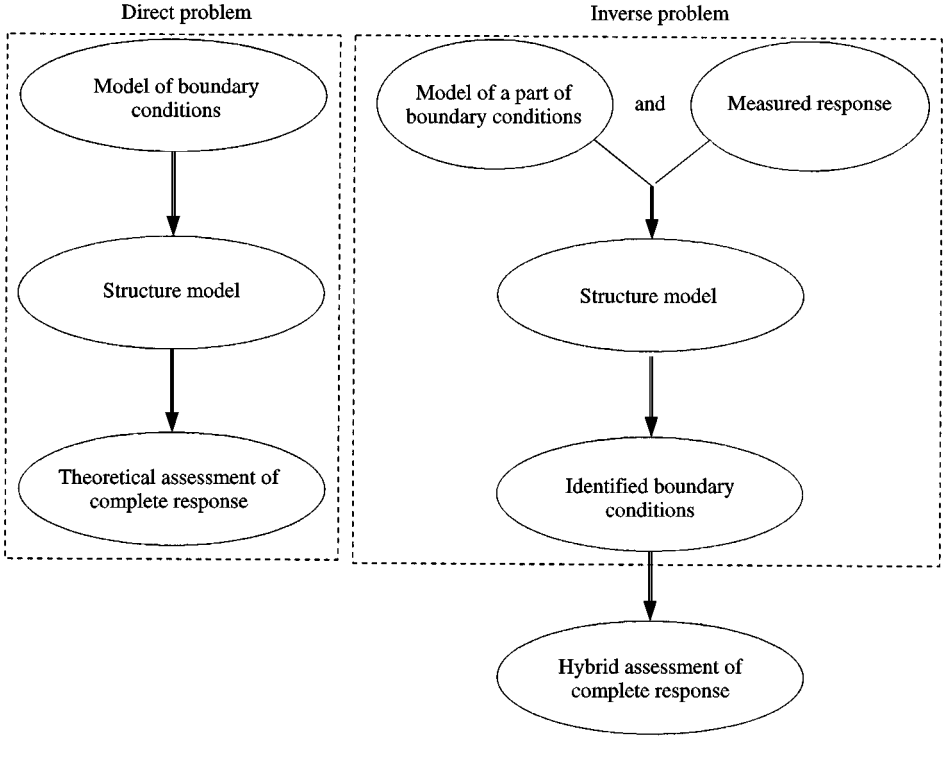

Figure 2. Direct and inverse problem.

response; its unknowns are the non-modelled boundary conditions and optionally the complete response of the system.

The dynamic behaviour of the tested system is assumed to be linear. Only steady state behaviour is considered so a frequency approach is used.

2.2. STRUCTURE MODEL

Elements and nodes are used to model the test part of the structure. Elements describe all the mechanical and geometrical properties. Nodes connect elements and make the junction between the modelled structure and those parts outside the test part.

Beam structures and piping systems are considered. At each point of a curvilinear element, a state vector composed of the generalized displacements $\{q\}$ and the generalized forces $\{Q\}$ can be defined. The structure model is based on a transfer matrix formulation which relates the dynamic state of one section of an element to the dynamic state of any other section. As an example, the classic transfer matrix of the Bernoulli straight beam is presented below. It is derived exactly from the motion equations

$$\rho S \frac{\partial^2 v}{\partial t^2} + EI \frac{\partial^4 v}{\partial x^4} = 0, \tag{1}$$

$$\theta_z = \frac{\partial v}{\partial x} \quad T_y = -EI \frac{\partial^3 v}{\partial x^3} \quad M_z = EI \frac{\partial^2 v}{\partial x^2}, \tag{2–4}$$

where ρ is the density, S is the cross-section area, EI is the flexural stiffness, T_y is the transverse shear force, M_z is the bending moment, v is the transverse displacement, and θ_z is the transverse rotation. The general solution $v(x, t)$ is expressed as follows:

$$v = (A e^{-jkx} + B e^{jkx} + C e^{-kx} + D e^{kx}) e^{j\omega t}, \quad k = \sqrt[4]{\frac{\rho S \omega^2}{EI}}, \tag{5}$$

where k is the wave number, ω is the angular frequency and (A, B, C, D) are the complex wave amplitudes.

The state vector definition at the ends of the element gives eight equations

$$T_1 = -T_y(x = 0), \qquad T_2 = T_y(x = L), \tag{6, 7}$$

$$M_1 = -M_z(x = 0), \qquad M_2 = M_z(x = L), \tag{8, 9}$$

$$v_1 = v(x = 0), \qquad v_2 = v(x = L), \tag{10, 11}$$

$$\theta_1 = \theta_z(x = 0), \qquad \theta_2 = \theta_z(x = L), \tag{12, 13}$$

where L is the length of the element. Note that T_1 and M_1 are, respectively, the transverse force and the bending moment applied to the beam by other parts of the structure. The elimination of wave amplitudes A, B, C and D in equations (6)–(13) leads to the dimensionles s transfer matrix for a given angular frequency ω:

$$\begin{Bmatrix} v_2 \\ \theta_2/k \\ T_2/k^3 EI \\ M_2/k^2 EI \end{Bmatrix} = \begin{bmatrix} a & c & d & b \\ -d & a & b & c \\ d & -b & -a & d \\ -b & -c & -c & -a \end{bmatrix} \begin{Bmatrix} v_1 \\ \theta_1/k \\ T_1/k^3 EI \\ M_1/k^2 EI \end{Bmatrix}, \tag{14}$$

where

$$a = \frac{\cos(kL) + \cosh(kl)}{2}, \qquad b = \frac{\cos(kL) - \cosh(kl)}{2}, \tag{15, 16}$$

$$c = \frac{\sin(kL) + \sinh(kl)}{2}, \qquad d = \frac{\sin(kL) - \sinh(kl)}{2}. \tag{17, 18}$$

In general, the dynamic behaviour of an element is expressed by a transfer matrix relationship:

$$\begin{Bmatrix} \mathbf{q}_2 \\ \mathbf{Q}_2 \end{Bmatrix} = \begin{bmatrix} \mathbf{T}_{qq} & \mathbf{T}_{qQ} \\ \mathbf{T}_{Qq} & \mathbf{T}_{QQ} \end{bmatrix} \begin{Bmatrix} \mathbf{q}_1 \\ \mathbf{Q}_1 \end{Bmatrix}, \tag{19}$$

where $\{\mathbf{q}_1\ \mathbf{Q}_1\}^{\mathrm{T}}$ is the state vector of the left extremity ($x = 0$), $\{\mathbf{q}_2\ \mathbf{Q}_2\}^{\mathrm{T}}$ is the state vector of the right extremity ($x = L$) and $[\mathbf{T}(\omega)]$ is the transfer matrix of the element. Other examples of transfer matrices of straight or curved tubes, with or without compressible fluids inside, having a constant or a varying cross-section, are developed in references [1,16–19].

Sensors are placed at nodes or in curvilinear elements. For sensors placed inside an element, the same formulation is used to relate experimental data to the structure degrees of freedom. Indeed, the transfer matrix $\mathbf{T}[x_s, \omega]$ relating the state vector of a sensor section ($x = x_s$) to the state vector of the element origin, is built up in the same manner as the element transfer matrix, only replacing the length of the element L by the curvilinear abscissa x_s:

$$\begin{Bmatrix} \mathbf{q}_s \\ \mathbf{Q}_s \end{Bmatrix} = [\mathbf{T}(x_s, \omega)] \begin{Bmatrix} \mathbf{q}_1 \\ \mathbf{Q}_1 \end{Bmatrix}. \tag{20}$$

A sensor can measure one or several components of the state vector of its cross-section. A selecting matrix $[\mathbf{A}_s]$ is used to extract the rows of the transfer matrix corresponding to the measured components $\{C_s\}$:

$$\{\mathbf{C}_s\} = [\mathbf{A}_s]\,[\mathbf{T}(x_s, \omega)] \begin{Bmatrix} \mathbf{q}_1 \\ \mathbf{Q}_1 \end{Bmatrix}. \tag{21}$$

Gathering all sensors at different positions of an element leads to the sensor transfer matrix relationship:

$$\{\mathbf{C}_e\} = \sum_k \mathbf{B}_k \mathbf{A}_{sk} \mathbf{T}(x_{sk}, \omega) \begin{Bmatrix} \mathbf{q}_1 \\ \mathbf{Q}_1 \end{Bmatrix} = [\mathbf{T}_s] \begin{Bmatrix} \mathbf{q}_1 \\ \mathbf{Q}_1 \end{Bmatrix}, \tag{22}$$

where $\{\mathbf{C}_e\}$ is the element sensor data, $[\mathbf{T}_s]$ is the measurement transfer matrix and $[\mathbf{B}_k]$ is an assembling matrix.

For each element a transfer relationship, including experimental data, is then obtained:

$$\begin{Bmatrix} \mathbf{q}_2 \\ \mathbf{Q}_2 \\ \mathbf{C}_e \end{Bmatrix}_{(\omega)} = \begin{bmatrix} \mathbf{T}_{qq} & \mathbf{T}_{qQ} \\ \mathbf{T}_{Qq} & \mathbf{T}_{QQ} \\ \mathbf{T}_{sq} & \mathbf{T}_{sQ} \end{bmatrix}_{(\omega)} \begin{Bmatrix} \mathbf{q}_1 \\ \mathbf{Q}_1 \end{Bmatrix}_{(\omega)}. \tag{23}$$

The assembling of transfer matrices is suitable for cascaded curvilinear elements without any bifurcation. For such substructures, it may be performed before assembling the whole structure. In this case, the resulting transfer matrix of the assembled substructure is the product of elementary transfer matrices. For the general case of three-dimensional networks including branched elements and bifurcations, an assembling procedure similar to finite element assembling technique is more suitable. To this end, equation (23) has to be transformed into a stiffness form where the generalized forces applied to the element and all the measurements performed on the element are expressed in terms of its extremities generalized displacements [20].

This transformation leads to

$$\begin{Bmatrix} \mathbf{Q}_1 \\ \mathbf{Q}_2 \\ \mathbf{C}_e \end{Bmatrix}_\omega = \begin{bmatrix} \mathbf{Z}^e_{11} & \mathbf{Z}^e_{12} \\ \mathbf{Z}^e_{21} & \mathbf{Z}^e_{22} \\ \mathbf{Z}^e_{s1} & \mathbf{Z}^e_{s2} \end{bmatrix}_\omega \begin{Bmatrix} \mathbf{q}_1 \\ \mathbf{q}_2 \end{Bmatrix}_\omega = \begin{bmatrix} -\mathbf{T}_{qQ}^{-1}\mathbf{T}_{qq} & \mathbf{T}_{qQ}^{-1} \\ \mathbf{T}_{Qq} - \mathbf{T}_{QQ}\mathbf{T}_{qQ}^{-1}\mathbf{T}_{qq} & \mathbf{T}_{QQ}\mathbf{T}_{qQ}^{-1} \\ \mathbf{T}_{sq} - \mathbf{T}_{sQ}\mathbf{T}_{qQ}^{-1}\mathbf{T}_{qq} & \mathbf{T}_{sQ}\mathbf{T}_{qQ}^{-1} \end{bmatrix} \begin{Bmatrix} \mathbf{q}_1 \\ \mathbf{q}_2 \end{Bmatrix}. \tag{24}$$

Easwaran [20] shows that, in the case of a conservative element, the dynamic stiffness matrix obtained from the transfer matrix is symmetric, which means that Z^e_{12} equals Z^e_{21}.

This transformation is not possible if the submatrix $[\mathbf{T}_{qQ}]$ is close to a singular matrix which occurs in the vicinity of the element's clamped-clamped eigenfrequencies. A simple subdivision of the element into two elements changes these eigenfrequencies and removes this singularity.

Classically, elementary dynamic stiffness matrices are assembled by connecting elements to nodes and expressing the conservation (momentum conservation for structure and mass conservation for fluid) and the continuity (displacement continuity for structure and pressure for fluid) equation for each node. A global sensor data vector $\{\mathbf{C}\}$ is formed, and the sensor data matrices $[\mathbf{Z}_{se}]$ are also assembled by connecting elements to nodes. This leads to a global equation expressing the generalized forces $\{Q\}$ and the measurements $\{\mathbf{C}\}$ in terms of the degrees of freedom $\{q\}$:

$$\begin{Bmatrix} \mathbf{Q} \\ \mathbf{C} \end{Bmatrix}_{(\omega)} = \begin{bmatrix} \mathbf{Z}_g \\ \mathbf{Z}_{sg} \end{bmatrix}_{(\omega)} \{\mathbf{q}\}_{(\omega)}. \tag{25}$$

The continuous elements formulation, where the motion equations are integrated in an exact manner, allows the dynamic behaviour of the system to be expressed using a small number of degrees of freedom. For example, a straight element, whatever its length, can be modelled using only one element. This formulation also has the advantage of allowing the introduction of measurements at any location of the network with the same accuracy.

2.3. BOUNDARY CONDITIONS

In predictive problems, a boundary condition is defined by knowing the generalized displacement or the generalized force or a relationship between them (impedance, reflection coefficient, etc.). Therefore, two classic types of boundary conditions are usually used: "clamped" where the displacement is known (modelled), and "free" where the force is known (null or modelled). All other classic boundary conditions can be modelled using a particular element described by a dynamic stiffness matrix.

Some of the boundary conditions are unknown. Thus, a new type of boundary condition has to be defined to make reference to the boundary degrees of freedom where neither

TABLE 1

Boundary condition types

Boundary condition	Generalized displacement	Generalized force
Link	Will be identified $\{q_l\}$	Will be identified $\{Q_l\}$
Imposed or clamped	Model data $\{q_c\}$	Unknown $\{Q_c\}$
Free or source	Unknown $\{q_f\}$	Model data $\{Q_f\}$

generalized forces nor generalized displacements are modelled. Both of them therefore have to be identified. This new type of boundary condition is referred to here as "link" degrees of freedom (Table 1).

2.4. CONDENSATION AND INVERSION

The unknowns in equation (25) are the link d.o.f. forces and displacements $\{\mathbf{q}_l\,\mathbf{Q}_l\}$, the free d.o.f. $\{\mathbf{q}_f\}$ and the reaction forces $\{\mathbf{Q}_c\}$ associated with clamped d.o.f. The number of equations is equal to the number of d.o.f. plus the number of sensors. Therefore, in order to get a full ranked system, the number of sensors must be at least equal to the number of link d.o.f. $\{\mathbf{q}_l\}$.

The inverse problem first aims to characterize the unknown boundary conditions by identifying $\{\mathbf{q}_l\}$ and/or $\{\mathbf{Q}_l\}$. In a preliminary stage, before solving equation (25), a condensa tion is performed in order to eliminate all other unknowns (associated with clamped and free d.o.f.). For this reason, the d.o.f. are sorted according to their boundary condition type:

$$\{\mathbf{q}\} = \{\{\mathbf{q}_l\}^t\ \{\mathbf{q}_f\}^t\ \{\mathbf{q}_c\}^t\}^t \quad \text{and} \quad \{\mathbf{Q}\} = \{\{\mathbf{Q}_l\}^t\ \{\mathbf{Q}_f\}^t\ \{\mathbf{Q}_c\}^t\}^t,$$

where subscript "l" denotes link d.o.f., "f" denotes free d.o.f., and "c" denotes clamped d.o.f. Equation (25) becomes

$$\begin{Bmatrix} \mathbf{Q}_l \\ \mathbf{Q}_f \\ \mathbf{Q}_c \\ \mathbf{C} \end{Bmatrix} = \begin{bmatrix} \mathbf{Z}_{ll} & \mathbf{Z}_{lf} & \mathbf{Z}_{lc} \\ \mathbf{Z}_{fl} & \mathbf{Z}_{ff} & \mathbf{Z}_{fc} \\ \mathbf{Z}_{cl} & \mathbf{Z}_{cf} & \mathbf{Z}_{cc} \\ \mathbf{Z}_{sl} & \mathbf{Z}_{sf} & \mathbf{Z}_{sc} \end{bmatrix} \begin{Bmatrix} \mathbf{q}_l \\ \mathbf{q}_f \\ \mathbf{q}_c \end{Bmatrix} \tag{26}$$

where subscript "s" denotes sensor data. The elimination of d.o.f. associated with unknowns $\{\mathbf{q}_f\}$ and $\{\mathbf{Q}_c\}$ leads to

$$\{\mathbf{Q}_l\} = [\mathbf{Z}_l]\{\mathbf{q}_l\} + \{\bar{\mathbf{Q}}_l\}, \qquad \{\mathbf{C}\} = [\mathbf{Z}_s]\{\mathbf{q}_l\} + \{\bar{\mathbf{C}}\}, \tag{27, 28}$$

where,

$$[\mathbf{Z}_l] = [\mathbf{Z}_{ll}] - [\mathbf{Z}_{lf}][\mathbf{Z}_{ff}]^{-1}[\mathbf{Z}_{fl}], \qquad [\mathbf{Z}_s] = [\mathbf{Z}_{sl}] - [\mathbf{Z}_{sf}][\mathbf{Z}_{ff}]^{-1}[\mathbf{Z}_{fl}], \tag{29, 30}$$

and

$$\{\bar{\mathbf{Q}}_l\} = [\mathbf{Z}_{lc}]\{\mathbf{q}_c\} + [\mathbf{Z}_{lf}][\mathbf{Z}_{ff}]^{-1}\{\mathbf{Q}_f\} \qquad \{\bar{\mathbf{C}}\} = [\mathbf{Z}_{sc}]\{\mathbf{q}_c\} + [\mathbf{Z}_{sf}][\mathbf{Z}_{ff}]^{-1}\{\mathbf{Q}_f\} \tag{31, 32}$$

The condensation presents two points of interest. The first advantage is that it allows the separation of the processing of modelled data $\{\mathbf{q}_c\}$ and $\{\mathbf{Q}_f\}$ from the processing of measured data $\{\mathbf{C}\}$. It is noted that the step involving measured data consists of solving a small linear system having a number of unknowns equal to the number of unknown boundary conditions.

The second advantage of condensation appears if this procedure is combined with a substructuring of the network. The condensation of modelled data may be achieved separately for each substructure, so that only small matrices are inverted.

These two advantages improve the conditioning of the inverse problem and reduce the sensitivity of the method to the data noise. Furthermore, this condensation does not introduce any loss of accuracy because the dynamic behaviour of the system is expressed using a physical and complete space (continuous elements model).

Equation (28) is solved to obtain the displacements $\{\mathbf{q}_l\}$. Overabundant measurements should be used in order to minimize the effects of errors caused by both limited accuracy of the measurements and the network modelling assumptions. A least-squares method [21,22], with a weighting matrix $[W]$, is used

$$\{\mathbf{q}_l\}_{(\omega)} = [[\mathbf{Z}_s]^{\mathrm{T}}[\mathbf{W}][\mathbf{Z}_s]]^{-1}\{[\mathbf{Z}_s]^{\mathrm{T}}[\mathbf{W}](\{\mathbf{C}\} - \{\bar{\mathbf{C}}\}). \tag{33}$$

Equation (27) gives the link generalized forces $\{\mathbf{Q}_l\}$:

$$\{\mathbf{Q}_l\}_{(\omega)} = [\mathbf{Z}_l]\,[[\mathbf{Z}_s]^{\mathrm{T}}[\mathbf{W}]\,[\mathbf{Z}_s]]^{-1}\{[\mathbf{Z}_s]^{\mathrm{T}}[\mathbf{W}](\{\mathbf{C}\} - \{\bar{\mathbf{C}}\})\} + \{\bar{\mathbf{Q}}_l\}. \tag{34}$$

The estimation of $\{\mathbf{q}_l\}$ or $\{\mathbf{Q}_l\}$ allows computation of the system response under actual test conditions. The complete response may be computed using a de-condensation procedur e which leads to the d.o.f. $\{\mathbf{q}_f\}$ and the reacting generalized forces $\{\mathbf{Q}_c\}$:

$$\{\mathbf{q}_f\} = [\mathbf{Z}_{ff}]^{-1}(\{\mathbf{Q}_f\} - [\mathbf{Z}_{fl}]\{q_l\} - [\mathbf{Z}_{fc}]\,\{\mathbf{q}_c\}), \tag{35}$$

$$\{\mathbf{Q}_c\} = [\mathbf{Z}_{cl}]\{\mathbf{q}_l\} + [\mathbf{Z}_{cf}]\{\mathbf{q}_f\} + [\mathbf{Z}_{cc}]\{\mathbf{q}_c\}. \tag{36}$$

The transfer matrix which relates a state vector of any section to its element d.o.f. allows the computation of displacements, strains and stresses at any location of the studied system.

This de-condensation procedure is also performed without any approximation and does not require a supplementary matrix computation.

Otherwise, $\{q_l\}$ and $\{Q_l\}$ may be used to model the boundary condition if a behaviour model of the connected element exists and has to be identified. In this case, the method proposed provides a local observation of the connected element from the measurement of the global response of the structure. Compared to a classic updating technique where the connected element is included in the structure, this approach provides a better conditioned inverse problem.

3. RESULTS

A computer program has been developed. It includes several continuous and lumped elements and provides a useful tool for inverse and predictive analysis of piping systems in the acoustic and vibration fields. The structure of the data entries and the processing algorithm are similar to those used in finite element programs.

The program and its several functionalities have been validated using a set of idealized tests which were successfully carried out. For these idealized tests, sensor data were

simulated without including any noise. In all cases tested, the agreement between the identified unknowns and those used to set-up the test simulation was perfect. The accuracy of the identification was equal to the numerical precision of the computer.

In order to test the feasibility and the efficiency of the method, several real tests have been carried out in the vibration and acoustics field. Three examples are presented here, the first is an academic test where some forces exciting a simple beam were measured and identified and where a simple supporting condition was identified. The two other examples provide real applications of the method. The second test was carried out in order to characterize a complex support used in nuclear plant piping systems. The third test was an application to piping system acoustics and was intended to analyze the behaviour of a branched resonator under realistic working conditions, when submitted to a turbulent grazing flow.

3.1. VALIDATION TEST

The validity of the method was first checked using a vibratory test bench (CAMELIA) developed by the Research Department of the French Electricity Company (EDF). It consisted of a circular straight pipe placed on two "V-form" supports. Two pieces of rubber inserted between the pipe and the supports insured a permanent contact and make the corresponding boundary conditions more linear, flexible and damped. The pipe was 3 m long and 2 mm thick, its external diameter was 42 mm. Two shakers were installed to excite the system. Forces applied by the shakers exciting the pipe and the corresponding accelerati on have been measured. These experimental data were only used to check the identification results. In addition, 16 accelerometers were distributed along the pipe as shown in Figure 3. They were used to identify boundary conditions, assumed to be unknown. The frequency band [5–391 Hz] which includes five eigenfrequencies (13–49–84–182–364 Hz) was investig ated.

The signals delivered by sensors were collected using a 40-channel signal analyser. Real-time processing provided the autopower of a reference channel and the cross-power of all the other channels with respect to the reference one. The Fourier spectrum of each channel, referenced in phase with respect to the reference channel was estimated as the ratio of the cross-power of the channel to the square root of the autopower of the reference channel.

Coherences were also computed and visualized, so as to control the linearity of the system and the signal/noise ratio of the measurements. In all cases, the obtained coherences were greater than 0·7 except for very low frequencies (< 10 Hz) and some single frequencies.

Several tests have been carried out with different excitations. A selection of obtained results is presented here. Table 2 describes these tests.

In all cases, the method presented above were used in order to identify the shaker excitations and end support conditions. Thus, the corresponding boundary conditions were assumed to be completely unknown. Only the pipe (AE) was modelled using Timoshenko beam continuous elements. Both supports were assumed to be punctual (no bending moment is applied on the pipe by the supports). In the case of the CAMELIA 2 configuratio n, the unknowns of the inverse problem were: the transverse displacements v_A, v_B, v_D, and v_E, and associated forces R_A, $F_B = F_1$, $F_D = F_2$ and R_E.

Several choices of sensors were tested. It was then established that five sensors (2, 7, 9, 10, 15) provided enough information to correctly identify the four unknown boundary conditio ns. Figure 4 gives a comparison between measured and identified forces F_1 and displacemen t v_A corresponding to the left shaker's d.o.f. Both graphs show a very good agreement between measured and identified unknowns, for frequencies greater than 20 Hz. These

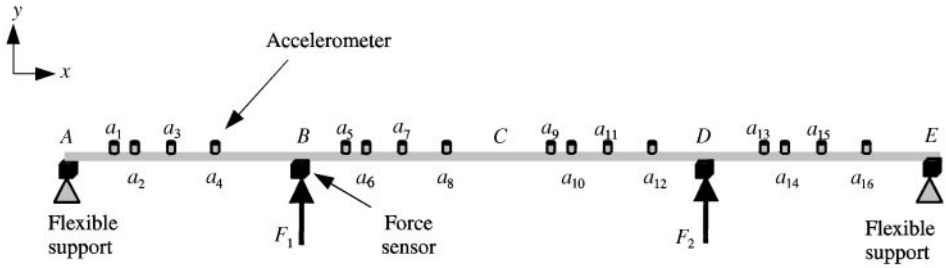

Figure 3. A schematic representation of the CAMELIA test bench.

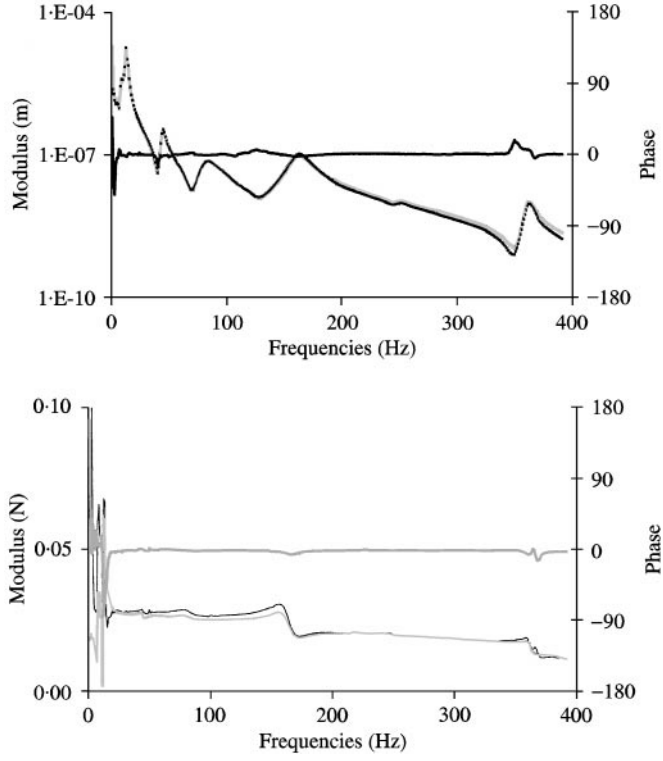

Figure 4. CAMELIA 2 results — identified and measured displacement (upper): (——) identified displacement; (——) measured displacement; and (——) phase, and force (lower); (——) identified force; (——) measured force; and (——) phase, corresponding to the left shaker boundary condition. The left axis corresponds to the modulus. The right axis corresponds to the phase difference between measured and identified force or displacement.

results are representative of data obtained from the set of tests which were carried out with this experimental set-up. The use of more overabundant sensors allowed a significant enhancement of the identification at low frequencies. Figure 5 shows that the left shaker force identified with 16 sensors is closer to the measured one than the force identified using only five sensors. In fact, the signals collected by the accelerometers were significantly noisy below 20 Hz; the use of more overabundant sensors reduced the noise effects.

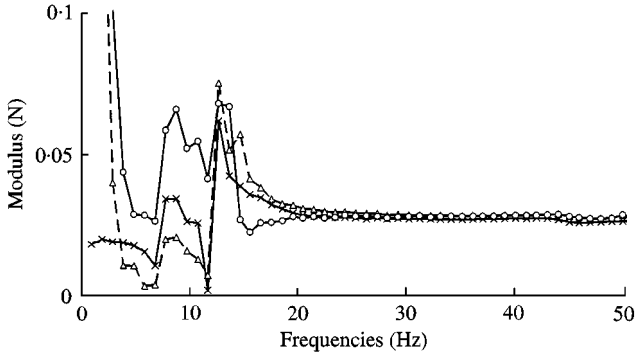

Figure 5. CAMELIA 2 results—influence of overabundant measurements for noisy low frequencies. Identified left shaker force using five sensors (–○–) is compared to that identified using 16 sensors (–△–) and the measured one (–×–).

TABLE 2

List of CAMELIA tests described

Test	Excitation configuration
CAMELIA 1	One white-noise excitation at point *D*: $F_1 = 0$; $F_2(\omega) = Cte$
CAMELIA 2	Two correlated in phase white-noise excitation at *B* and *D*
CAMELIA 3	Two opposite phase white-noise excitations at *B* and *D*

The support dynamic stiffness of end supports has also been examined. The identification of bending moments M_A and M_E applied to the pipe by the supports shows that they can be neglected when compared to the associated transverse forces R_A and R_E. Therefore, each support/pipe connection can be modelled by a one-degree-of-freedom reactive link. The corresponding dynamic stiffness may be estimated by the ratio of the identified transverse force to the identified transverse displacement ($\mathbf{Z}_A = R_A/v_A$; $Z_E = R_E/v_E$). The left support dynamic stiffness Z_A obtained in three tests (see Table 2) are compared. Although the supports were not excited in the same manner due to different test configurations, Figure 6 shows a good agreement between the corresponding identified stiffnesses. It is particularly noted that the two opposite phase excitations test does not excite the same eigenmodes as the two correlated in phase excitations test. The real part of the stiffness exhibits a parabolic form, which can be compared with a mass–spring behaviour, and the imaginary part is a nearly straight line, which characterizes the support damping.

The case where the user cannot safely predict the location or the origin of a vibrating source was also examined. Some free d.o.f. should then be declared as unknown boundary conditions. In order to examine the ability of the method to locate actual excitations and links, the identification was performed in the CAMELIA 2 configuration supposing that there was another unknown excitation or connection at the middle of the pipe (point C). Additional unknowns v_C and F_C were then introduced. Figure 7 shows that the identificatio n of the real excitation F_B remains very close to that measured. The fictitious identified force F_C was very low compared to the real one. This means that the method is able to locate the real excitations at points B and D.

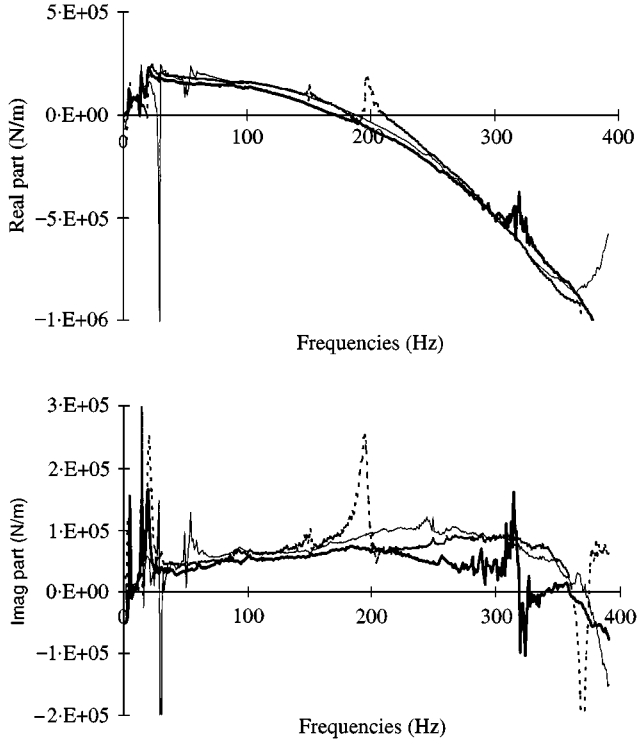

Figure 6. Dynamic stiffness of the left support. Upper: Real part—Lower: imaginary part CAMELIA 1 (—), CAMELIA 2 (——), CAMELIA 3 (– – –).

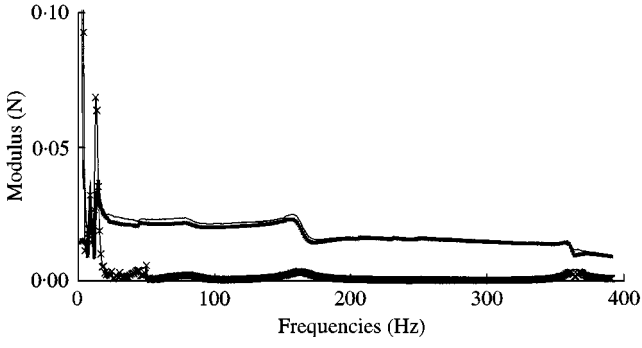

Figure 7. Influence of a fictitious link boundary condition. Configuration CAMELIA 2. (—) measured excitation; (——) identified actual excitation and (-×-) fictitious force.

In this method, it was assumed that the test structure was well known. Thus, sensitivity of the identified boundary conditions against inaccuracies in the model of the test structure was investigated. The configuration CAMELIA 2 was considered, and Young's modulus of the pipe was assumed equal to $2{\cdot}1 \times 10^5$ MPa instead of $1{\cdot}85 \times 10^5$ MPa. A fictitious unknown link was also added at the middle of the pipe (point C). In order to avoid the errors due to the measurement noise, an overabundant number of sensors was used.

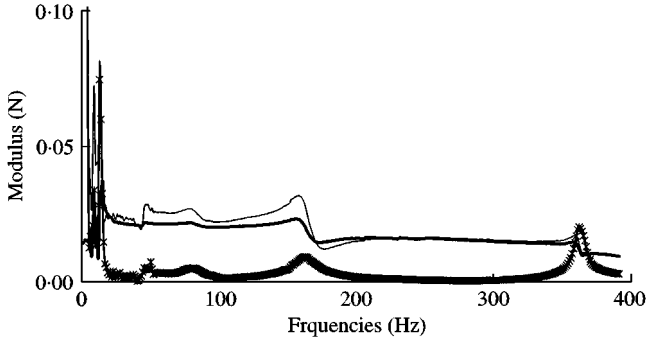

Figure 8. Influence of a tested structure model error. Configuration CAMELIA. Fictitious force corresponding to the link boundary condition added at the middle of the pipe (-×-) compared to identified (——) and measured (—) shaker force.

Figure 8 shows the identified shaker force F_B compared to the measured one and the identified fictitious force F_C. Compared to the results in Figure 7, a significant identification error can be observed. This result shows that it is important to use an accurate model of the test structure. It is also shown here that the magnitude of the fictitious force may be used to detect the model inaccuracies and the resulting effects on the identified boundary conditions.

All these results proved the feasibility and the efficiency of the identification method. The case of two correlated forces was particularly interesting as it showed the ability of the approach also to locate correlated vibratory sources. The characterization of the support stiffness was also performed for a set of different and uncontrolled excitations. The agreement between results obtained shows the ability of the method to characterize the support behaviour in real functioning conditions. The following example focuses on this point.

3.2. PIPING SUPPORT CHARACTERIZATION

This test gives an industrial example. The developed method was used to analyze and characterize an example of complicated supporting conditions of a nuclear power plant piping system: the cross-wall support. A laboratory test stand was constructed. A freely suspended straight pipe of 5·5 m length was attached to the support 2·4 m from its upstream end and was submitted to an uncontrolled excitation. The excitation and support resisting forces were measured. The support was composed of a clamping collar fixed on a steel frame (Figure 9). A force sensor was placed between the frame and the collar and thus it did not measure exactly the resisting force applied to the pipe by the collar.

Seventeen accelerometers were used to identify the excitation force, the support force and bending moment, and the resisting forces at the extremities of the pipe (suspended by elastic bands). Figure 10 compares the measured and identified excitation. One can see that, except for a few narrow bands where identified force shows some wrong peaks, the shaker force was correctly identified. Figure 11 shows the same result for the identified support resisting force. For frequencies lower than 150 Hz, the identified resisting force was in good agreeme nt with that measured. A significant disagreement was noticed for higher frequencies. In fact, this difference between the measured and identified force was caused by the inertia of

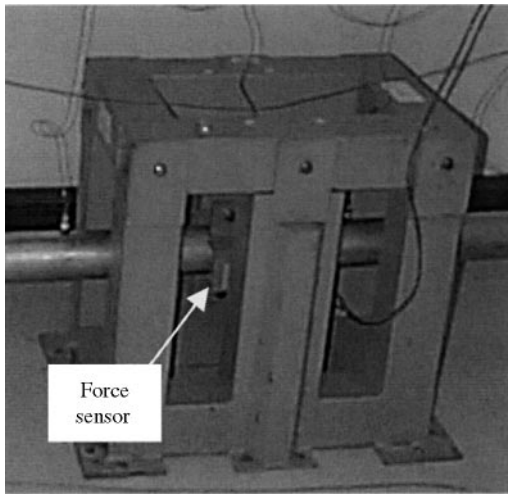

Figure 9. Cross-wall support test stand.

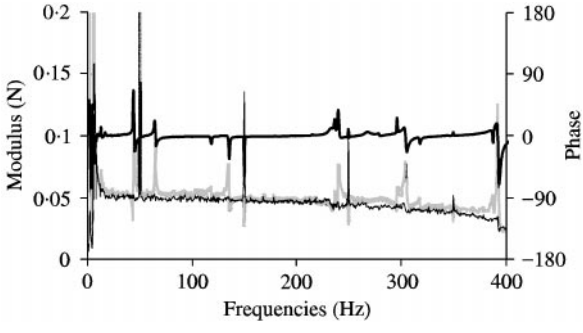

Figure 10. Cross-wall support characterization test — identified excitation compared to measured one. Left axis: modulus. Right axis: phase difference between identified and measured force. (——) identified excitation; (——) measured excitation; and (—) phase.

the collar. The static stiffness of the support was very high, so, at low frequencies, displacement and acceleration of the collar remained very low and the corresponding inertia forces could be neglected. In contrast, when the frequency increased, the velocity of the collar also increased and the collar kinematic energy became non-negligible.

It was not possible to insert the sensor between the collar and the pipe to measure accurately the resisting force. The sensor was actually measuring the force applied by the frame to the collar. This means that the identified force was more reliable than that measured and closer to the actual force. This provides an example where the use of the inverse method becomes necessary.

Figure 12 shows the real part of the supporting dynamic stiffness. It shows that the first support eigenfrequency is about 312 Hz. This frequency is a consequence of the geometrical and mechanical characteristics of the support and of the mechanical behaviour of the assembly. Modelling the latter is generally a difficult task because it often depends on linking conditions (working gap, clamping ranges, etc.). Other eigenfrequencies appear

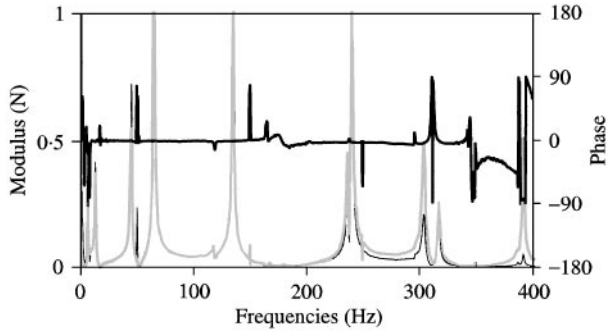

Figure 11. Cross-wall support characterization test—identified support resisting force compared to that measured. Left axis: modulus. Right axis: phase difference between identified and measured force. (——) identified resisting forct; (——) measured resisting force; and (—) phase.

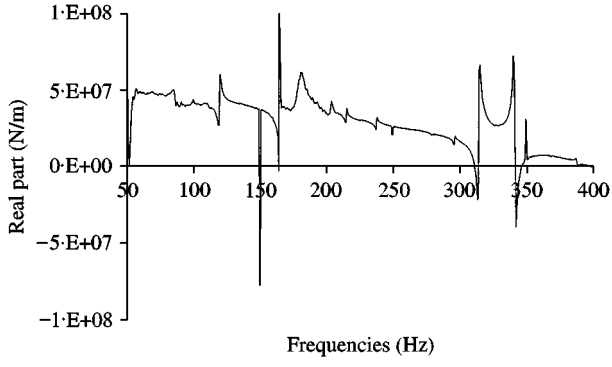

Figure 12. Dynamic stiffness of cross-wall supporting.

when examining this dynamic stiffness (119, 164, 203, 215, 238, 296 Hz). They correspond to some local eigenmodes of the support.

3.3. BRANCHED RESONATOR CHARACTERIZATION

The developed method has also been tested in the acoustic field. The feature of this test is that the experimentation was carried out in order to investigate a physical phenomenon occurring at the interface between a main pipe and a branched singularity. The method is useful because it provides a close observation of the interface behaviour without performing any intrusive measurements.

A test stand was constructed in order to analyze the effects of grazing flow on branched resonators. The test system was composed of a 5 m test tube including a branched Helmholtz resonator connected to the laboratory high-pressure network (Figure 13). The grazing flow was turbulent and fully developed. The aim of the study was to investigate the local aero-acoustic coupling at the interface between the main pipe and the resonator. This coupling may strongly affect the quality factor of the resonator and modify its resonance frequency.

The pipe between the first microphone and the right end was modelled. A transfer matrix taking into account the viscous dissipation and the flow effects was used [19]. The open end

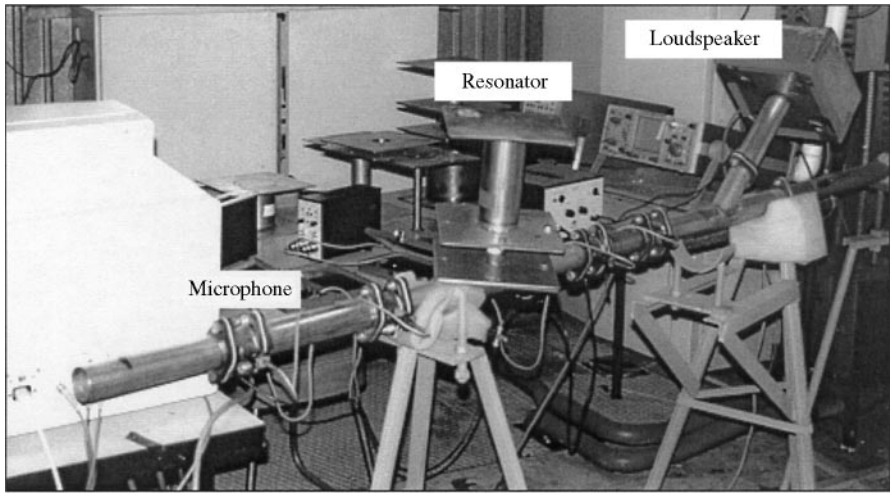

Figure 13. Branched Helmholtz Resonators — the resonator is composed of a branched neck and a volume. Downstream of the resonator, one can see the loudspeaker (sloped upstream box) providing an acoustic excitation inside the pipe and the connection with the laboratory high-pressure flow network.

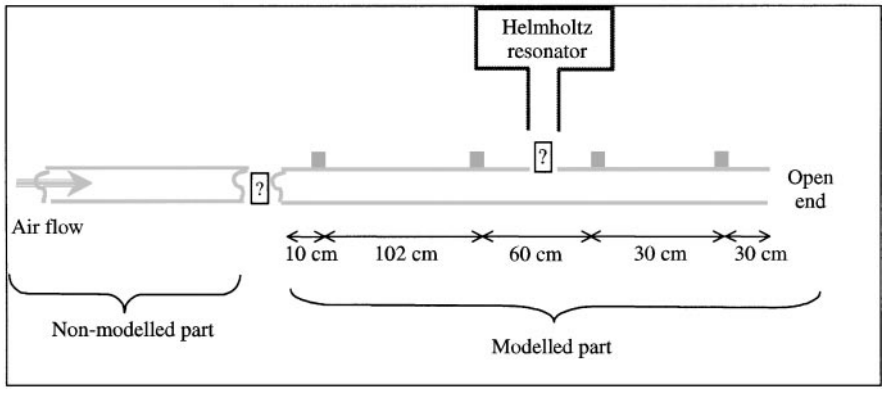

Figure 14. Schematic diagram of the flow testing stand used to identify the acoustic pressure and velocity at the entry of the Helmholtz resonator submitted to a turbulent grazing flow. "?" indicates unknown boundary conditions.

of the pipe is modelled using the Levine–Schwinger's model [23]. The resonator was assumed to be completely unknown. The corresponding boundary condition was then considered as a "link" boundary condition. Otherwise, the mean flow involved some unknown sources in the upstream part of the test pipe, so the boundary conditions at the entry of the test pipe could neither be controlled nor modelled and had to be identified (Figure 14).

Two flush mounted B&K $\frac{1}{4}''$ microphones were placed on either side of the branched resonator to measure the internal acoustical pressure. The corresponding experimental data were used in the identification procedure.

Figure 15 shows the identified impedance for several mean flow speeds. The nominal resonance frequency of the resonator was about 270 Hz. Some known effects of mean flow

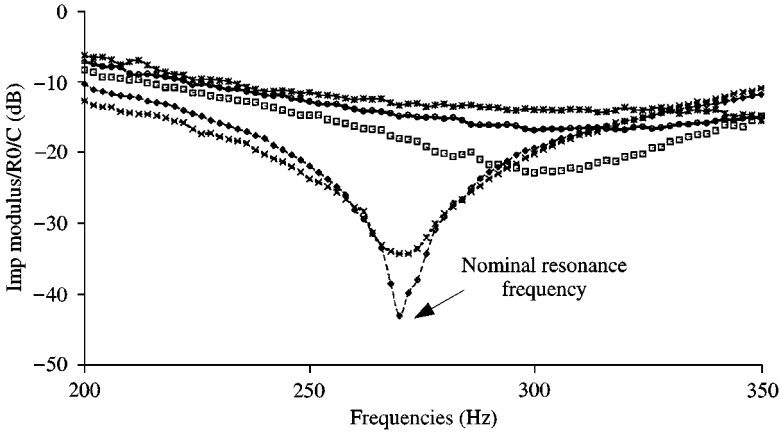

Figure 15. Identified impedance of a Helmholtz resonator submitted to a grazing flow normalized by the specific impedance of the media (ρc). (–×–) Mach 0; (–◆–) Mach 0·05; (□) Mach 0·1; (–○–) Mach 0·15; and (–■–) Mach 0·2.

can be observed: shift of resonance frequency and increasing of damping effects. This proves the reliability of the results. The entry impedance of a set of 25 resonators was identified. Currently, these results are being investigated for analyzing and modelling the grazing flow effects at the entry of a branched tube.

4. CONCLUSION

In the field of experimental analysis of operating systems, a new method of boundary condition identification has been presented. It concerns the case where only a part of an analyzed system is tested and where the interface conditions with the rest of the system and dynamic sources generated inside are nither modelled nor controlled. Unknown boundary conditions make predicting the response of the system a difficult problem to define. In this paper, it is shown that the measurement of the response of the system at a few internal points removes the weakness of the problem and replaces the lack of inputs.

The first stage, and the main aim of the method presented, consists of the characterization of the dynamic state of the system boundary. Since unknown boundary conditions are identified, a diagnosis or a predictive analysis may be performed. Otherwise the characteriza tion of the boundary condition may address the analysis of the singular behaviour of the boundary subsystem. In this case, the test structure is used as a non-intrusive macro-sensor providing some information on the connected subsystem. The identification of boundary conditions leads to a local observation of the singularity behaviour.

This method compliments the existing methods which are based on wave intensity measurement and on experimental modal analysis. It has the advantage that it can be applied to three-dimensional curvilinear structures. An inverse problem is solved where the target boundary conditions (inputs) are globally expressed in terms of the measured response (outputs) in the frequency domain.

The developments discussed are focused on piping system network analysis. In this case, the use of an exact transfer matrix is shown to be very suitable. In fact, it allows the system behaviour to be expressed without any discretization error and leads to a few d.o.f. in the analytical model. Furthermore, the condensation of the modelled boundary conditions

allows the model data and experimental data to be separated when solving the inverse problem, which improves its conditioning.

Several experimental tests are presented in the paper. The first is an academic test which is performed in order to check the feasibility and the validity of the approach. The results show the efficiency of the method when identifying generalized forces and displacement associated with an unknown boundary condition. The results also show that the method allows the characterization of the reactive boundary condition without any significant dependence on the excitation of the tested system.

The second and the third tests provide some practical examples. The support characteriza tion test is an industrial case where the usefulness of the method for *in situ* characterization in industrial environment is shown. The third test provides an example of a laboratory application where a physical phenomenon has to be analyzed without making intrusive measurements.

REFERENCES

1. S. Frikha 1992 Analyse expérimentale des sollicitations dynamiques appliquées à une portion de structure en service modélisable par la théorie des poutres. *Ph.D. thesis ENSAM—Paris.*
2. D. J. Ewins 1990 *Modal Testing Theory and Practice.* London: Research Studies Press Ltd.
3. J. N. Juang and R. S. Papa 1985 *AIAA Journal of Guidance, Control and Dynamics* **8**, 620–627. An eigensystem realization algorithm for modal parameters identification and model reduction.
4. P. Ladeveze, D. Nedjar, and M. Reynier 1994, *AIAA Journal* **32**, 1485–1491. Updating of finite element model using vibration tests.
5. M. I. Friswell and J. E. Mottershead 1995 *Finite Element Model Updating in Structural Dynamics.* Dordrecht: Kluwer Academic Publishers.
6. J. E. Mottershead and M. I. Friswell 1993 *Journal of Sound and Vibration* **162**, 347–375. Model updating in structural dynamics: a survey.
7. H. G. Natke 1988 *Probabilistic Engineering Mechanics* **3**, 28–35. Updating computational models in the frequency domain based on measured data: a survey.
8. S. R. Ibrahim 1990 *Journal of Vibrations and Acoustics* **112**, 107–111. A direct Two response approach for updating analytical dynamic model of structure with emphasis on uniqueness.
9. M. W. Lesmez, D. C. Wiggert and F. J. Hatfield 1990 *Transaction of the ASME Journal of Fluids Engineering* **112**, 311–318. Modal analysis of vibrations in liquid-filled piping systems.
10. L. Hermans and H. V. Der Auverar 1997 *Proceedings of the* 15*th International Modal Analysis Conference, Orlando*, FL. Modal parameter extraction from in-operation data.
11. G. H. James, T. G. Carne and J. P. Laufer 1995 *International Journal of Analytical and Experimental Modal Analysis* **10**, 260–277. Natural excitation technique (NExT) for modal parameter extraction from operating structures.
12. G. Pavic 1993 *Journal of Sound and Vibration* **49**, 221–230. Measurement of structure borne intensity, Part I: formulation of the methods.
13. A. Causse and J. L. Trolle 1988 *Proceedings of InterNoise Conference Avignon*, France. Analysis of nuclear plant circuit by vibrational intensity measurement.
14. A. F. Seybert 1988 *Journal of the Acoustical Society of America* **83**, 2233–2239. Two sensor methods for the measurement of sound intensity and acoustic property in ducts.
15. L. Mongeau 1995 *Journal of Sound and Vibration* **181**, 369–389. A method for characterising aerodynamic sound sources in turbo-machines.
16. E. Dokumaci 1999 *Journal of Sound and Vibration* **217**, 869–882. An exact transfer matrix formulation of plane sound wave transmission in inhomogeneous ducts.
17. E. C. Pestel and F. A. Leckie, 1963 *Matrix Method in Elastomechanics.* New York: Mc Graw Hill Book Co.
18. L. Meirovitch 1967 *Analytical Methods in Vibrations.* New York: Macmillan.
19. M. L. Munjul 1987 *Acoustics of Ducts and Mufflers.* New York: John Wiley.
20. V. Easwaran, V. H. Gupta and M. L. Munjal 1993 *Journal of Sound and Vibration* **161**, 515–525. Relation between the impedance matrix and the transfer Matrix with specific reference to reciprocal and conservative systems.

21. G. H. GOLUB and C. F. VAN LOAN 1990 *Matrix Computation*. Baltimore, MD: John Hopkins University Press, Mathematics/Computer Science, second edition.
22. J. E. DENNIS, 1977 *Non Linear Least Squares and Equations—State of the Art in Numerical Analysis*. New York: Academic Press.
23. M. LEVINE and J. SCHWINGER 1948 *Physical Review* **73**, 383–406. On the radiation of sound from unflanged circular pipe.

APPENDIX A: NOMENCLATURE

$\{\mathbf{C}\}$	measured response
$\{\bar{\mathbf{C}}\}$	source term following condensation of $\{Q_f\}$ and $\{q_c\}$ in the measurement transfer matrix
EI	flexural stiffness
k	wave number
M_{fz}	bending moment
$\{\mathbf{q}\}$	generalized kinematic co-ordinates (linear or angular position for structure, acoustical pressure for gas and liquid)
$\{\mathbf{q}_c\}$	clamped d.o.f.
$\{\mathbf{q}_f\}$	free d.o.f.
$\{\mathbf{q}_l\}$	d.o.f. having an unknown boundary condition
$\{\mathbf{Q}\}$	generalized forces (forces and moments for structure, acoustical flow for gas and liquid)
$\{\mathbf{Q}_c\}$	reacting generalized forces associated with clamped d.o.f.
$\{\mathbf{Q}_f\}$	modelled excitation, generalized forces associated with free d.o.f.
$\{\mathbf{Q}_l\}$	unknown generalized forces corresponding to an unknown boundary condition
$\{\bar{\mathbf{Q}}_l\}$	source term following condensation of $\{q_f\}$ and $\{q_c\}$ in the dynamical stiffness matrix
S	cross-section area
$[\mathbf{T}]$	transfer matrix
T_y	transverse shear force
$[\mathbf{W}]$	weighting matrix
$[\mathbf{Z}]$	dynamic stiffness matrix
$[\mathbf{Z}_l]$	dynamic stiffness matrix condensed to link d.o.f.
$[\mathbf{Z}_s]$	measurement/d.o.f. transfer matrix condensed to link d.o.f.
v	transverse displacement
ρ	density
θ_z	transverse rotation.
$\{\mathbf{\Theta}\}$	state vector
ω	angular frequency.